

Whale Optimization Algorithm with Constriction Factor and Amplitude Matching Technology for Real Time Lower Order Modelling

N.Malathi, N.Devarajan

Abstract: Recently developed Whale Optimization Algorithm (WOA) has been enhanced in this paper with Constriction Factor (CF) to clench up the random exploration in the search trajectory. The WOA with CF is experimented by multidimensional benchmark functions and validated in terms of optimum solution and convergence speed. Then it is employed to determine few unknown parameters in the lower order modelling of Linear Time Invariant Discrete Systems (LTIDS) and Linear Time Invariant Continuous Systems (LTICS) for minimum Internal Square Error (ISE) in which, the other unknown parameters were estimated by Laurent-series based amplitude matching technology. The proposed method is implemented to few real systems including Multi Input Multi Output (MIMO) systems.

Keywords: Whale Optimization Algorithm, Constriction Factor, lower order modelling, Amplitude matching, ISE, LTICS, LTIDS, MIMO.

I. INTRODUCTION

Optimization is to solve practical problems by obtaining the best result with minimal effort in any given domain. It's a potent tool to be applied in our everyday life in a variety of situations and problems. Based on the application, the problem to be solved for can be a minimization or maximization problem. In the Engineering domain, optimization means gaining the maximum profit, the best design, optimum routing or controlling with the least production effort/cost. The nature of the real-time optimization problems is often very involved with many constraints, so, various algorithms and their variants have been developed to solve them.

The population-based foraging in species like ants, birds, and whales exhibits highly coordinated behavior and increased intelligence as a group or swarm. This is due to shared information among the swarm by various methods of interaction. Vibrations may establish interactions as in fishes, chemical traces and flock in birds, etc. By this way, the millions of years of nature's evolution is demonstrating an effective intelligent method to solve a problem.

Revised Manuscript Received on April 15, 2019.

N.Malathi, Research Scholar, Dept of Electrical Eng., Centre for Research ,Anna University, Chennai, Tamil Nadu, India.

N.Devarajan, Dean-Research, Sri Ramakrishna Institute of Technology, Coimbatore, Tamil Nadu, India.

Nature inspired metaheuristic algorithms are considered authoritative and most adopted for their simplicity and efficacy. The list includes Evolutionary algorithm, Particle Swarm Optimization (PSO), Cuckoo search algorithm, Ant Colony Optimization, Artificial Bee Colony Algorithm and so on. The discovery of error minimization technique leads to adopting the intelligent optimization algorithms for order reduction. Hence, recently developed, bio-inspired, population-based WOA is improved in this work with Constriction Factor and employed for tuning the lower order model coefficients.

II. WHALE OPTIMIZATION ALGORITHM

Stimulated by the world's biggest mammals, Seyedali Mirjalili and Andrew Lewis developed a metaheuristic algorithm in 2016 called Whale Optimization Algorithm [1]. WOA involves a swarm of agents searching for the best solution and its position by employing 'Bubble-net' attacking technique of humpback whales, which includes shrinking encircling, spiral updating and random exploration for prey. The leader/best-solution agent's position is defined, and it is assumed as the closest position to the optimum-value/prey. Whales always encircle the prey once spotted. A mathematical model of encircling mechanism for other search agents to update their positions towards the best solution agent is given by Position overhaul towards an optimum solution:

$$\vec{D} = |\vec{C} \cdot \vec{X}^*(t) - \vec{X}(t)| \quad (1)$$

$$\vec{X}(t+1) = \vec{X}^*(t) - \vec{A} \cdot \vec{D} \quad (2)$$

where, t – current iteration; \vec{A}, \vec{C} – coefficient vectors; $\vec{X}(t)$ – the position of the search agent; $\vec{X}^*(t)$ – the position of the best-solution agent;

$$\vec{A} = 2\vec{a} \cdot \vec{r} - \vec{a} \quad (3)$$

$$\vec{C} = 2 \cdot \vec{r} \quad (4)$$

\vec{a} – distance control parameter, linearly decreases from 2 to 0; \vec{r} – random number [0,1]. Variable \vec{a} is has diminishing value to accomplish the shrinking encircling mechanism of bubble net attacking technique. The spiral strategy is realized by mimicking the 9-shaped spiral movement of humpback whales in terms of using the spiral equation for search agent's position update.

$$\vec{D}' = |\vec{X}^*(t) - \vec{X}(t)| \quad (5)$$



$$\vec{X}(t+1) = \vec{D}' \cdot e^{bl} \cos(2\pi l) + \vec{X}^*(t) \quad (6)$$

where b – constant defines the shape of a logarithmic spiral; l – random number in $[-1, 1]$.

Exploration for prey: Humpback whales search randomly for the prey. By choosing a random position, the current agent whale is forced to move far away from the current leader whale/best solution and search for a new best. Hence a global exploration is assured. The random position overhaul model is given by

$$\vec{D}_{rand} = |\vec{C} \cdot \vec{X}_{rand} - \vec{X}(t)| \quad (7)$$

$$\vec{X}(t+1) = \vec{X}_{rand} - \vec{A} \cdot \vec{D}_{rand} \quad (8)$$

Establishing Bubble-net attacking technique: By nature, the humpback whales swim around the prey in “9” shaped spiral path, which is shrinking simultaneously. To model this, [2] assumed a 50% likelihood of selecting shrinking-encircling and spiral strategy for the overhaul of search agent’s position. An arbitrary number p is introduced. Where p – in the range of $[0, 1]$. Shrinking technique is established if $p < 0.5$, else spiral strategy is called out. To establish the random search exploration and obtain the global optimizer, the coefficient vector \vec{A} is utilized. In the current search cycle, if $\vec{A} \geq 1$, the random search will be called out. If $p \geq 0.5$, search agent’s position is overhauled by spiral strategy. $\vec{X}(t+1)$ is obtained by (5) and (6). If $p < 0.5$ and $\vec{A} < 1$, search agent’s position is overhauled by shrinking encircling strategy with respect to the current best solution. $\vec{X}(t+1)$ is obtained by (1), (2), (3) and (4). If $p < 0.5$ and $\vec{A} \geq 1$, position adjustment is done by random exploration. $\vec{X}(t+1)$ is obtained by (7), (8), (3) and (4).

III. IMPROVED WHALE OPTIMIZATION ALGORITHM WITH CONSTRICTION FACTOR (CF)

Though the conventional WOA gives satisfactory results, many attempts such as introducing inertia weight by Hu & Xu [3] adaptive technology by Jangir et.al. [4] and correction factors by Siva lingam et.al. [5] were made in the past to improve the convergence and search space.

Swarm intelligent techniques, which employ exploration and exploitation may tend to diverge and go unstable, called as explosion in Particle Swarm Optimization (PSO) technique. Velocity constraint incorporated in the PSO failed to improve the fine search whereas it can prevent the explosion. To balance the exploration and explosion behaviour and ensure the convergence, Clerc and Kennedy formulated Constriction Factor in their studies on the explosion, stability and convergence in PSO [6]. After works show that the CF approach with PSO generates higher quality solutions [7], [8] and [9]. WOA algorithm which also employs exploration strategy is not incorporated with either velocity or inertia weight to accelerate the stable convergence. Inspired by PSO, the CF is incorporated with WOA in this thesis. As per the mathematical theory [6] of CF, it doesn’t virtually modify the fundamental equation of the algorithm. They proposed the CF formulation which is valid only when inertia weight is 1 [10]. Hence the implementation of CF for WOA becomes straightforward. The constriction factor developed for the best convergence by Clerc and Kennedy after analyzing the deterministic particle member’s trajectory is given by

$$CF = \chi = \frac{2\kappa}{|2 - \phi - \sqrt{\phi^2 - 4\phi}|} \quad (9)$$

Where $0 < \kappa \leq 1$. Kappa (κ) mostly gets the value 1. And $\phi \geq 4$. Now the WOA with CF, improved distance and position equations of encircling, spiral strategy and random exploration become

$$\vec{D}_{CF} = CF * (|\vec{C} \cdot \vec{X}^*(t) - \vec{X}(t)|) \quad (10)$$

$$\vec{X}(t+1) = \vec{X}^*(t) - \vec{A} \cdot \vec{D}_{CF} \quad (11)$$

$$\vec{D}_{CF}' = CF * (|\vec{X}^*(t) - \vec{X}(t)|) \quad (12)$$

$$\vec{X}(t+1) = \vec{D}_{CF}' \cdot e^{bl} \cos(2\pi l) + \vec{X}^*(t) \quad (13)$$

$$\vec{D}_{rand.CF} = CF * (|\vec{C} \cdot \vec{X}_{rand} - \vec{X}(t)|) \quad (14)$$

$$\vec{X}(t+1) = \vec{X}_{rand} - \vec{A} \cdot \vec{D}_{rand.CF} \quad (15)$$

Implementation of WOA with CF as follows:

Step 1: The number of search agents is assumed ($i=1,2,3,...n$). The best solution agent’s fitness cost is initialized as ∞ for maximization and $-\infty$ for a minimization problem. The positions of search agents are randomly assigned. Some search variables, upper and lower bounds of search variables and maximum iteration are initialized.

Step 2: Fitness cost function for all the search agents are calculated. If the lowest fitness is encountered, then its position and fitness cost are assigned as the best solution variables.

Step 3: To establish Bubble-net technique, every search agent for every variable’s positions are overhauled by considering constants A and p as in the case of conventional WOA. If $p \geq 0.5$, overhaul by spiral strategy. $\vec{X}(t+1)$ is obtained by (9), (12) & (13). If $p < 0.5$ and $\vec{A} < 1$, overhaul by shrinking encircling. $\vec{X}(t+1)$ is obtained by (9), (10), (11), (3) and (4). If $p < 0.5$ and $\vec{A} \geq 1$, position adjustment by random exploration. $\vec{X}(t+1)$ is obtained by (9), (14), (15), (3) and (4).

Step 4: Increment the iteration count by 1 and check if the max iteration is reached. If the count is less than max, then perform step2, step3, and step4. If the max iteration is reached, then the best solution variables are declared as an optimum value.

13 multidimensional unconstraint benchmark functions are tested, to validate the feasibility and performance of the WOA with CF.

1. Sphere function $f_1 = \sum_{i=1}^n x_i^2$; dimension: 30; limit: $-100 \leq x_i \leq 100$.
2. Schwefel 2.22 $f_2 = \sum_{i=1}^n |x_i| + \prod_{i=1}^n |x_i|$; dimension: 30; limit: $-10 \leq x_i \leq 10$.
3. Schwefel 2.21 function $f_3 = \max\{|x_i|, 1 \leq i \leq n\}$; dimension: 30; limit: $-100 \leq x_i \leq 100$.
4. Rosenbrock’s function $f_4 = \sum_{i=1}^{n-1} [100(x_{i+1} - x_i^2)^2 + (x_i - 1)^2]$; dimension: 30; limit: $-30 \leq x_i \leq 30$.
5. Step function $f_5 = \sum_{i=1}^n (|x_i + 0.5|)^2$; dimension: 30; limit: $-100 \leq x_i \leq 100$.
6. Sphere function $f_6 = \sum_{i=1}^4 ix_i^4 + rand()$; dimension: 30; limit: $-1.28 \leq x_i \leq 1.28$.
7. function $f_7 = -\sum_{i=1}^n x_i \sin \sqrt{|x_i|}$; dimension: 30; limit: $-500 \leq x_i \leq 500$.

8. function $f_8 = \sum_{i=1}^n (x_i^2 - 10 \cos(2\pi x_i) + 10)$;
dimension: 30; limit: $-5.12 \leq x_i \leq 5.12$.
9. function $f_9 =$
 $-20 \exp\left(-0.2 \sqrt{\frac{1}{n} \sum_{i=1}^n x_i^2}\right) - \exp\left(\frac{1}{n} \sum_{i=1}^n \cos(2\pi x_i)\right) + 20 + e$;
dimension: 30 ; limit : $-100 \leq x_i \leq 100$.
10. function $f_{10} = \frac{1}{4000} \sum_{i=1}^n x_i^2 - \prod_{i=1}^n \cos\left(\frac{x_i}{\sqrt{i}}\right) + 1$;
dimension: 30; limit: $-600 \leq x_i \leq 600$.
11. function $f_{11} = 4x_1^2 - 2.1x_1^4 + \frac{1}{3}x_1^6 + x_1x_2 - 4x_2^2 + 4x_2^4$; dimension: 30; limit: $-5 \leq x_i \leq 5$.
12. function $f_{12} = \left(x_2 - \frac{5.1}{4\pi^2} x_1^2 + \frac{5}{\pi} x_1 - 6\right)^2 + 10 \left(1 - \frac{1}{8\pi}\right) \cos x_1 + 10$; dimension: 30; limit: $-5 \leq x_i \leq 5$.
13. function $f_{13} = [1 + (x_1 + x_2 + 1)^2(19 - 14x_1 + 3x_1^2 - 14x_2 + 6x_1x_2 + 3x_2^2)[30 + (2x_1 - 3x_2)2(18 - 32x_1 + 12x_1^2 + 48x_2 - 36x_1x_2 + 27x_2^2)]$;dimension: 30;limit : $-2 \leq x_i \leq 2$.

The computation results of 13 functions are shown below.

Table. 1 Best Solution for Benchmark Functions

Function	WOA with CF	WOA
f1	5.2757x10⁻⁰⁴²	5.1226x10 ⁻⁰³⁸
f2	1.8494x10⁻⁰²⁷	2.7805x10 ⁻⁰²⁴
f3	9.0682	53.4008
f4	26.9446	27.8812
f5	0.5791	0.13859
f6	0.0084941	0.0026196
f7	-8626.1219	-8628.1137
f8	0	0
f9	7.9936x10⁻⁰¹⁵	2.2204x10 ⁻⁰¹⁴
f10	0	0
f11	-1.0316	-1.0316
f12	0.39789	0.39789
f13	3	3

The convergence curve for all 13 functions are shown below

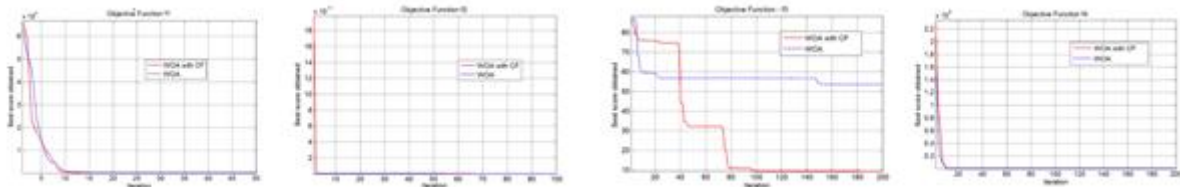


Fig. 1 Convergence of f1,f2,f3 and f4 with WOA & WOA with CF

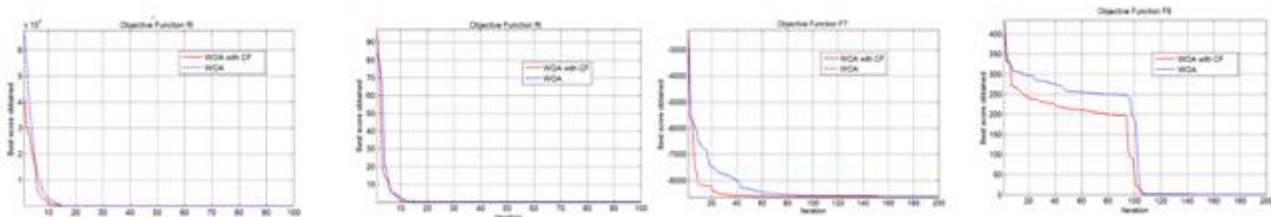


Fig. 2 Convergence of f5,f6,f7 and f8 with WOA & WOA with CF

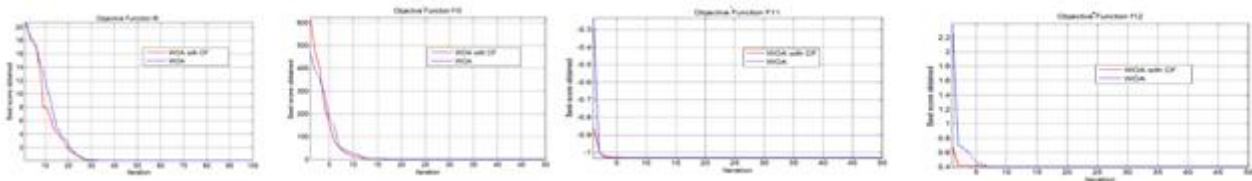


Fig. 3 Convergence of f9,f10, f11 and f12 with WOA & WOA with CF

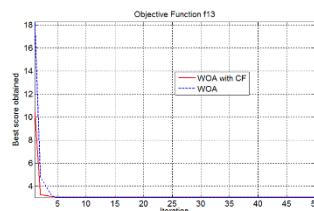


Fig. 4 Convergence f13 with WOA & WOA with CF

IV. MODEL REDUCTION - AMPLITUDE MATCHING

Real-time systems are always characterised as mathematical models for the ease of analysis and design.

These mathematical models can be the equations in terms of one or more variables.

Such equations become intricate when they are modelled closer to reality. Nevertheless, such complicated systems may increase the computation time. To reduce the computational intricacy, lower order models are formulated to replicate their original intricate models and preserve significant dynamics. One among the classical methods is amplitude matching scheme[11] [12], in which the amplitudes of original higher order system and reduced order systems at various time indexes are matched to obtain a few parameters of equivalent reduced order model. The discovery of error minimization technique leads to adopting the intelligent optimization algorithms for lower order modelling. Hence, the remaining parameters are obtained by WOA with CF. If required, the numerator and denominator orders of the reduced order model can be changed.

A. LTIDS

Let the stable original higher order and reduced second order LTIDS are

$$G(z) = \frac{N(z)}{D(z)} = \frac{\sum_{i=0}^m a_i z^i}{\sum_{i=0}^n b_i z^i} = \frac{a_m z^m + a_{m-1} z^{m-1} + \dots + a_0}{b_n z^n + b_{n-1} z^{n-1} + \dots + b_0} \quad \text{and} \quad R(z) = \frac{k_1 z + k_0}{z^2 + l_1 z + l_0} \quad (16)$$

Where $m < n$; a_i ($0 \leq i \leq m$), b_i ($0 \leq i \leq n$), k_1 , k_0 , l_1 , and l_0 are scalar constants. From [11] and [12], for $m=n-1$ matching the amplitude at first time index and steady state gives $R(z) = \frac{a_1 z + [\alpha_{ss}(1+l_1+l_0)-a_1]}{z^2 + l_1 z + l_0}$. Where $\alpha_1 = k_1 = \frac{a_{n-1}}{b_n}$ and $\alpha_{ss} = \frac{k_1 + k_0}{1+l_1+l_0} = \frac{\sum_{i=0}^{n-1} a_i}{\sum_{i=0}^n b_i}$. The unknown parameters l_1 and l_0 are obtained by invoking the WOA with CF for minimum ISE. For $m \neq n-1$, amplitude matching at first time index and steady state gives $R(z) = \frac{k_1 z + [\alpha_{ss}(1+l_1+l_0)-k_1]}{z^2 + l_1 z + l_0}$ where k_1 , l_1 and l_0 are determined by WOA with CF.

B. LTICS

Let the stable original higher order and reduced second order LTICS are

$$G(s) = \frac{\sum_{i=0}^m A_i s^i}{\sum_{i=0}^n B_i s^i} = \frac{A_m s^m + A_{m-1} s^{m-1} + \dots + A_0}{B_n s^n + B_{n-1} s^{n-1} + \dots + B_0} \quad \text{and} \quad R(s) = \frac{K_1 s + K_0}{s^2 + L_1 s + L_0} \quad (17)$$

where $m < n$; A_i ($0 \leq i \leq m$), B_i ($0 \leq i \leq n$), K_1 , K_0 , L_1 and L_0 are scalar values; Then for $m=n-1$; $R(s) = \frac{\alpha_1 s + (\alpha_{ss}(L_0))}{s^2 + L_1 s + L_0}$ and for $m \neq n-1$; $R(s) = \frac{K_1 s + \alpha_{ss}(L_0)}{s^2 + L_1 s + L_0}$ where, $\alpha_1 = K_1 = \frac{A_m}{B_n}$ and $\alpha_{ss} = \frac{K_0}{L_0} = \frac{A_0}{B_0}$. The unknown values are determined by WOA with CF.

C. MIMO Systems

Any MIMO system can be represented in terms of subsystem transfer functions. The output equation of a two input two output MIMO LTIDS is given as

$$\begin{bmatrix} Y_1(z) \\ Y_2(z) \end{bmatrix} = \begin{bmatrix} \frac{Q_{11}(z)}{\Delta(z)} & \frac{Q_{12}(z)}{\Delta(z)} \\ \frac{Q_{21}(z)}{\Delta(z)} & \frac{Q_{22}(z)}{\Delta(z)} \end{bmatrix} \begin{bmatrix} U_1(z) \\ U_2(z) \end{bmatrix} = \begin{bmatrix} G_{11}(z) & G_{12}(z) \\ G_{21}(z) & G_{22}(z) \end{bmatrix} \begin{bmatrix} U_1(z) \\ U_2(z) \end{bmatrix} \quad (18)$$

$Q_{ik}(z)$ is the numerator polynomials of the subsystems and $\Delta(z)$ is the characteristic polynomial of the MIMO LTIDS. $G_{11}(z) = \frac{a_m z^m + a_{m-1} z^{m-1} + \dots + a_0}{b_n z^n + b_{n-1} z^{n-1} + \dots + b_0}$ and $R_{11}(z) = \frac{k_1 z + k_0}{z^2 + l_1 z + l_0}$. For $m=n-1$; $R_{11}(z) = \frac{a_1 z + [\alpha_{ss}(1+l_1+l_0)-a_1]}{z^2 + l_1 z + l_0}$. For $m \neq n-1$, $R_{11}(z) = \frac{k_1 z + [\alpha_{ss}(1+l_1+l_0)-k_1]}{z^2 + l_1 z + l_0}$. The unknown values are obtained by WOA with CF. Similarly, individual other subsystem transfer functions $G_{12}(z)$, $G_{21}(z)$,.... can be taken from (18) and the corresponding reduced order models $R_{12}(z)$, $R_{21}(z)$... are formulated.

The output equation of a two input two output MIMO LTICS is represented as,

$$\begin{bmatrix} Y_1(s) \\ Y_2(s) \end{bmatrix} = \begin{bmatrix} \frac{N_{11}(s)}{\Delta(s)} & \frac{N_{12}(s)}{\Delta(s)} \\ \frac{N_{21}(s)}{\Delta(s)} & \frac{N_{22}(s)}{\Delta(s)} \end{bmatrix} \begin{bmatrix} U_1(s) \\ U_2(s) \end{bmatrix} = \begin{bmatrix} G_{11}(s) & G_{12}(s) \\ G_{21}(s) & G_{22}(s) \end{bmatrix} \begin{bmatrix} U_1(s) \\ U_2(s) \end{bmatrix} \quad (19)$$

$N_{ik}(s)$ is the numerator polynomials of the subsystems and $\Delta(s)$ is the characteristic polynomial of the MIMO LTICS. The first subsystem transfer function $G_{11}(s) = \frac{A_m s^m + A_{m-1} s^{m-1} + \dots + A_0}{B_n s^n + B_{n-1} s^{n-1} + \dots + B_0}$ and $R_{11}(s) = \frac{K_1 s + K_0}{s^2 + L_1 s + L_0}$. For $m=n-1$; $R_{11}(s) = \frac{\alpha_1 s + (\alpha_{ss}(L_0))}{s^2 + L_1 s + L_0}$. For $m \neq n-1$, $R_{11}(s) = \frac{K_1 s + \alpha_{ss}(L_0)}{s^2 + L_1 s + L_0}$. In which the unknown values are obtained by WOA with CF. Similarly, other individual subsystem transfer functions $G_{12}(s)$, $G_{21}(s)$,.... can be mined from (19) and the corresponding reduced order models $R_{12}(s)$, $R_{21}(s)$... are formulated.

V. ILLUSTRATIONS

A. Example 1

Consider the transfer function of a digital IIR filter in lattice ladder structure as shown in Figure 5. $H(z) = \frac{1+2z^{-1}+2z^{-2}+z^{-3}}{1+\frac{13}{24}z^{-1}+\frac{5}{8}z^{-2}+\frac{1}{3}z^{-3}} = \frac{z^3+2z^2+2z+1}{z^3+0.5416z^2+0.625z+0.333}$ [13].

The proposed reduction technique is used to reduce the delay units in the IIR filter structure. The $H(z)$ lattice ladder coefficients are $k_0 = 0.2500$; $k_1=0.5001$; $k_2= 0.3330$. $c_0= -0.2694$; $c_1= 0.8280$; $c_2= 1.4584$ and $c_3=1.0000$.

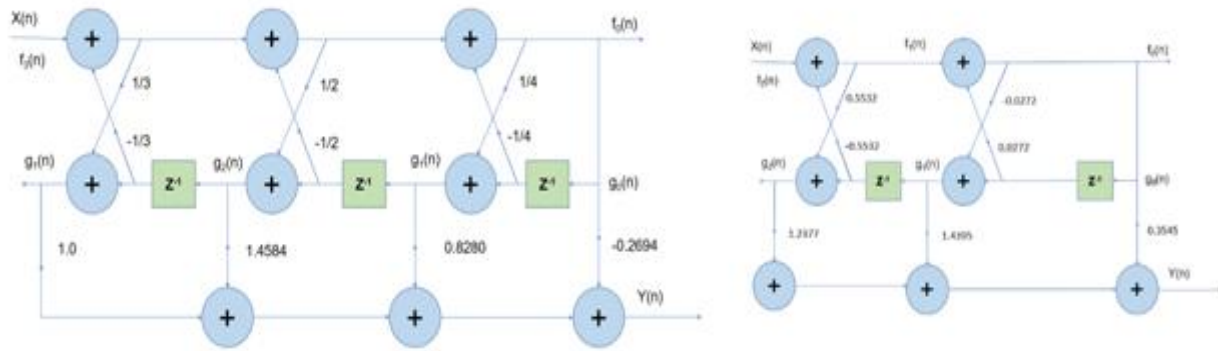


Fig. 5 Higher Order and Proposed Reduced order IIR Filter Structure in Lattice Ladder Form

The order reduction of $H(z)$ is obtained by the proposed method. $R(z)$ is compared in Table II, Figure 6 and Figure 7.

Table. 2 ISE Comparison of Reduced Order Models - Example 1

Method	Reduced Order Model	ISE for 0.4 unit time.
Ramesh Model [13]	$R(z) = \frac{1.537z^2 + 2.414z + 2.049}{1.537z^2 + 0.174z + 0.7863}$	0.1061
Gomathi Model [14]	$R(z) = \frac{0.8551z^2 + 1.632z + 0.7769}{z^2 - 0.1171z + 0.4769}$	0.1015
Proposed Method	$R(z) = \frac{1.7164z^2 + 2.3809z + 2.1244}{1.7164z^2 - 0.0726z + 0.9495}$	0.0306

The reduced order filter lattice ladder coefficients are $k_{r0} = -0.0272$; $k_{r1} = 0.5532$. $c_{r1} = 0.3545$; $c_{r2} = 1.4395$; $c_{r3} = 1.2377$ and the lattice ladder structure is shown in Figure 5.

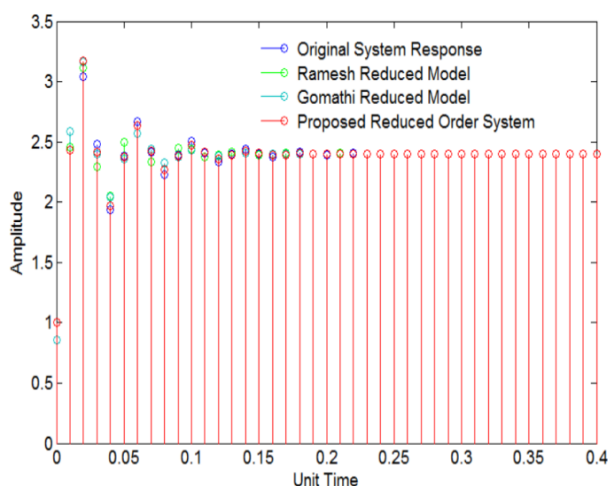


Fig. 6 Comparison of Step Responses

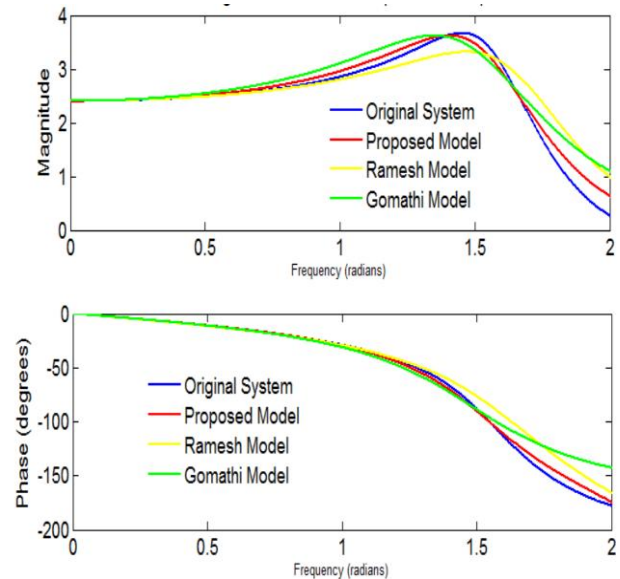


Fig. 7 Comparison of Magnitude and Phase Responses

It is observed that the proposed reduced order IIR filter gives better approximation regarding step response ISE and frequency response.

B. Example 2

Considering the Phillips -Heffron model of the single-machine infinite- bus practical power system (a standard IEEE type-1 exciter) as in Figure 8. Referring the system modelling and data from [15], 3-phase Synchronous machine 160 MVA, $\text{pf} = 0.894$, $x_d = 1.7$, $x_q = 1.6$, $x_d' = 0.245$ p.u., $\tau_{do} = 5.9$, $H = 5.4$ s, $\omega_R = 314$ rad/s. Exciter : $K_A = 50$, $K_F = 0.04$, $K_R = K_0 = 1$, $K_E = -0.17$, $S_E = 0.95$, $\tau_A = 0.05$, $\tau_E = 0.95$, $\tau_F = 1$, $\tau_R = 0.05$, $\tau_0 = 10$, $\tau_1 = \tau_3 = 0.440$, $\tau_2 = \tau_4 = 0.092$ s. External System : $X_e = 0.40$, $R_e = 0.02$ p.u. (160 MVA base). Operating-Point : $P_0 = 1$, $Q_0 = 0.5$, $E_{FD0} = 2.5128$, $E_{q0} = 0.9986$, $v_{t0} = T_{m0} = 1$ p.u., $\delta_0 = 1.1966$ rad, $K_1 = 1.1330$, $K_2 = 1.3295$, $K_3 = 0.3072$, $K_4 = 1.8235$, $K_5 = -0.0433$, $K_6 = 0.4777$.

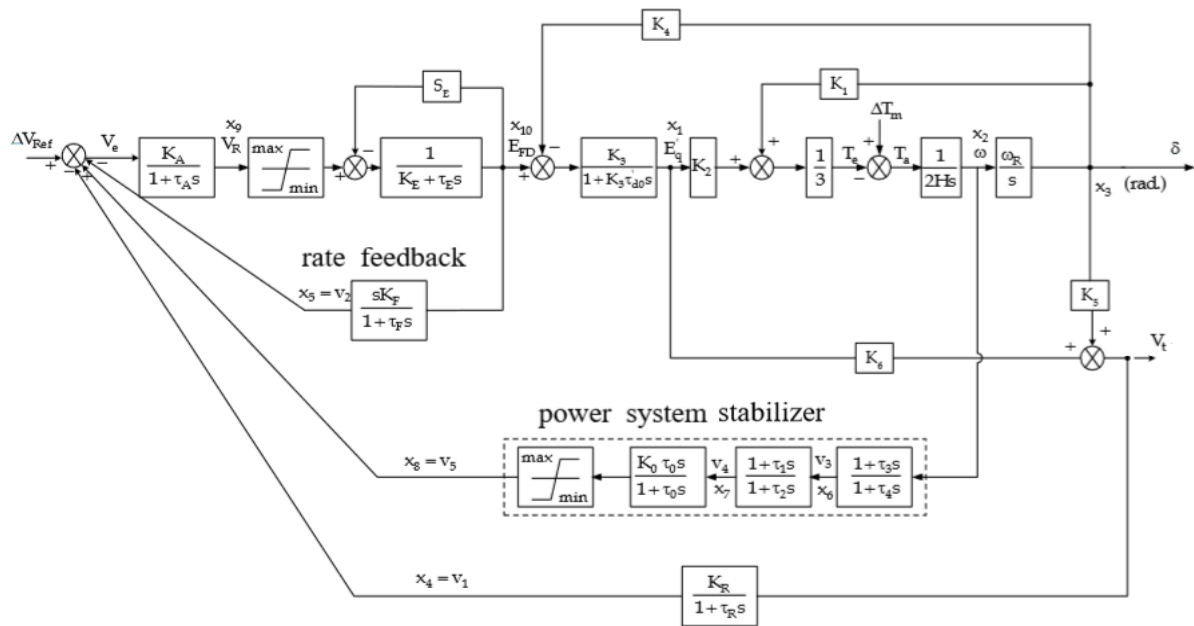


Fig. 8 Representation of Phillips -Heffron model of the single-machine infinite- bus power system

$$\begin{aligned} \begin{bmatrix} \delta \\ V_t \end{bmatrix} &= \begin{bmatrix} a & b \\ c & d \end{bmatrix} \begin{bmatrix} \Delta V_{ref} \\ \Delta T_m \end{bmatrix} = G_{ij}(s) \begin{bmatrix} \Delta V_{ref} \\ \Delta T_m \end{bmatrix} = \frac{1}{D(s)} \begin{bmatrix} N_{11}(s) & N_{12}(s) \\ N_{21}(s) & N_{22}(s) \end{bmatrix} \begin{bmatrix} \Delta V_{ref} \\ \Delta T_m \end{bmatrix}, \text{ where,} \\ D(s) &= s^{10} + 64.21s^9 + 1596s^8 + (1.947 \times 10^4 s^7) + (1.268 \times 10^5 s^6) + (5.036 \times 10^5 s^5) + (1.569 \times 10^6 s^4) \\ &\quad + (3.24 \times 10^6 s^3) + (4.061 \times 10^6 s^2) + (2.095 \times 10^6 s) + 2.531 \times 10^5 \\ N_{11}(s) &= -(2298s^5) - (9.85 \times 10^4 s^4) - (1.38 \times 10^6 s^3) - (6.838 \times 10^6 s^2) - (6.1 \times 10^6 s) - 5.43 \times 10^5 \\ N_{12}(s) &= 29.09s^8 + 1868 s^7 + (4.61 \times 10^4 s^6) + (5.459 \times 10^5 s^5) + (3.185 \times 10^6 s^4) + (8.702 \times 10^6 s^3) \\ &\quad + (1.206 \times 10^7 s^2) + (7.606 \times 10^6 s) + 6.483 \times 10^5 \\ N_{21}(s) &= 85.23 s^7 + 3651s^6 + (5.208 \times 10^4 s^5) + (2.98 \times 10^5 s^4) + (8.471 \times 10^5 s^3) + (3.105 \times 10^6 s^2) \\ &\quad + (2.752 \times 10^6 s) + 2.45 \times 10^5 \\ N_{22}(s) &= -1.26s^8 - 85.18 s^7 - 2089 s^6 - (2.568 \times 10^4 s^5) - (1.909 \times 10^5 s^4) - (7.123 \times 10^5 s^3) \\ &\quad - (1.084 \times 10^6 s^2) - (2.972 \times 10^5 s) - 1.942 \times 10^4 \end{aligned}$$

Individual transfer function models are $G_{ij}(s) = \frac{N_{ij}(s)}{D(s)}$. Where $i=j=1,2$ for the given two input two output system. Their corresponding reduced order models after the proposed amplitude matching are $R_{ij}(s) = \frac{K_{1s+SS(L_0)}}{s^2+L_1s+L_0}$. $R_{11}(s) = \frac{K_{1s-2.1439(L_0)}}{s^2+L_1s+L_0}$; Now the WOA with CF is invoked to obtain the three unknown values. Keeping the $R_{11}(s)$ denominator as a common denominator, the unknown K_1 values in R_{12} , R_{21} and R_{22} are determined. The sub system reduced order models are $R_{11}(s) = \frac{3.6209s-10.9831}{s^2+1.3025s+5.1194}$, $R_{12}(s) = \frac{8.3419s+13.1135}{s^2+1.3025s+5.1194}$, $R_{21}(s) = \frac{-0.9863s+4.95575}{s^2+1.3025s+5.1194}$, and $R_{22}(s) = \frac{-0.8563s-0.39277}{s^2+1.3025s+5.1194}$.

Table. 3 ISE Comparison of Reduced Order Models - Example 2

Vishwakarma Model[16]	ISE	Salma Model [17]	ISE	Proposed Model	ISE
$R_{11}(s)$ $= \frac{8.8 s^2 - 64.35 s - 20.1}{s + 10.03 s^2 + 32.28 s + 9.37}$	299.9964	$R_{11}(s)$ $= \frac{7.07 s^2 - 18.24 s - 2.49}{s^3 + 0.5785 s^2 + 10.5690 s + 1.0}$	1017.9	$R_{11}(s)$ $= \frac{3.6209 s - 10.9831}{s^2 + 1.3025 s + 5.11}$	87.3813
$R_{12}(s)$ $= \frac{38.27 s^2 + 88.78 s + 24}{s^3 + 10.03 s^2 + 32.28 s + 9.37}$	1135.5	$R_{12}(s)$ $= \frac{0.68 s^2 + 29.97 s + 2.5}{s^3 + 0.5785 s^2 + 10.5690 s + 1.0}$	72.8822	$R_{12}(s)$ $= \frac{8.3419 s + 13.1135}{s^2 + 1.3025 s + 5.11}$	595.1154
$R_{21}(s)$ $= \frac{-3.03 s^2 + 29 s + 9.1}{s^3 + 10.03 s^2 + 32.28 s + 9.37}$	20.5115	$R_{21}(s)$ $= \frac{-0.78 s^2 + 7.9 s + 1.2}{s^3 + 0.5785 s^2 + 10.5690 s + 1.0}$	114.7338	$R_{21}(s)$ $= \frac{-0.9863 s + 4.9557}{s^2 + 1.3025 s + 5.11}$	9.0050
$R_{22}(s)$ $= \frac{7.27 s^2 - 5.23 s - 0.72}{s^3 + 10.03 s^2 + 32.28 s + 9.37}$	18.7980	$R_{22}(s)$ $= \frac{-0.02 s^2 - 2.4 s + 0.03}{s^3 + 0.5785 s^2 + 10.5690 s + 1.0}$	10.0825	$R_{22}(s)$ $= \frac{-0.8563 s - 0.3927}{s^2 + 1.3025 s + 5.11}$	8.8419

Table III compares the ISE of each subsystem of the given power system. Figure 9 gives the response of δ when $\Delta V_{ref}(s)=0.05$ p.u and $\Delta T_m(s)=0$ and the step response of V_t when $\Delta V_{ref}(s)=0.05$ p.u and $\Delta T_m(s)=0$. Similarly, Figure 10 displays the step responses of δ and V_t when $\Delta V_{ref}(s)=0$

and $\Delta T_m(s)=0.05$ p.u. From the Figures, it is noticed that the proposed method results sufficiently closer step response to that of their original higher order system. The proposed method produces overall improved results when compared to the existing methods referred here.

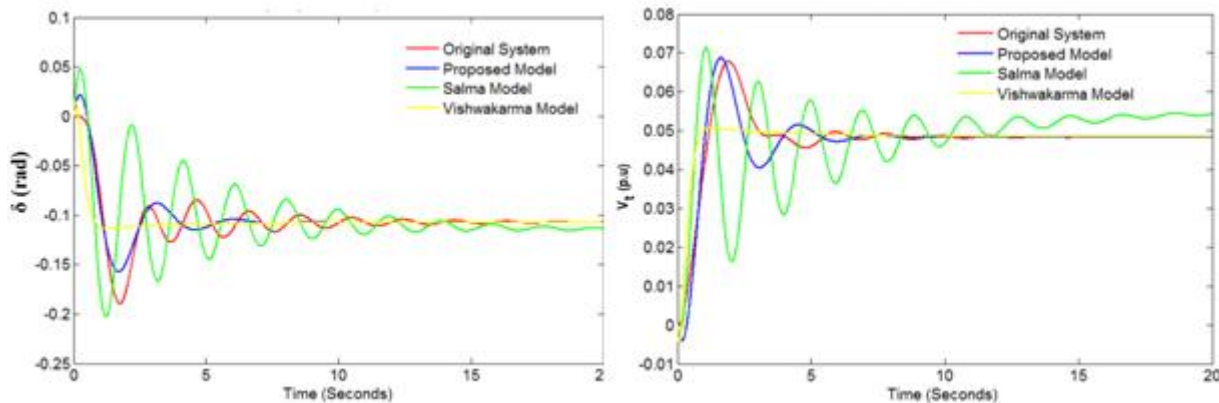


Fig. 9 Response of δ when $\Delta V_{ref}(s)=0.05$ p.u & $\Delta T_m(s)=0$ and Response of V_t when $\Delta V_{ref}(s)=0.05$ p.u & $\Delta T_m(s)=0$

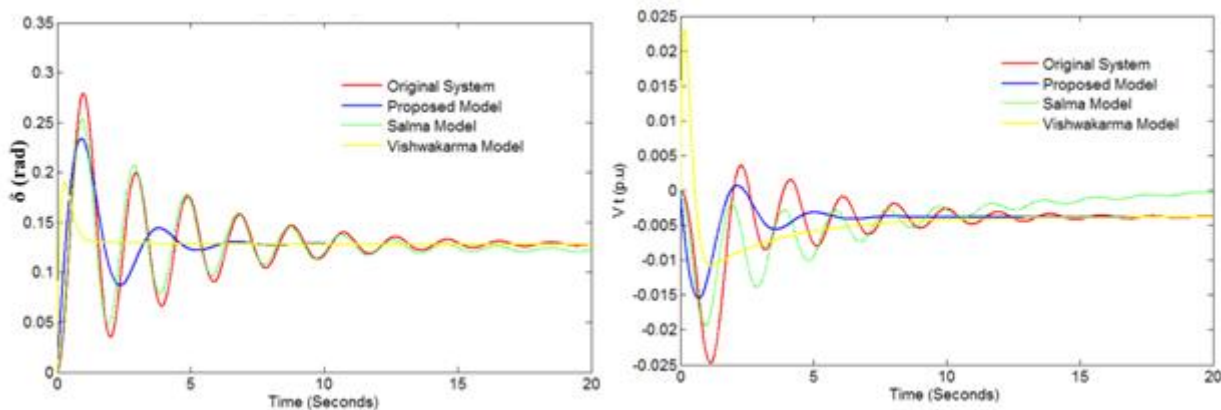


Fig. 10 Response of δ when $\Delta V_{ref}(s)=0$ & $\Delta T_m(s)=0.05$ p.u and Response of V_t when $\Delta V_{ref}(s)=0$ & $\Delta T_m(s)=0.05$ p.u

C. Example 3

The model of an aircraft azimuth channel blind landing system is taken for lower order approximation. The block diagram of the aircraft control system is shown in Figure 11. With forward gain K in degree/foot; Aircraft-autopilot time constant $T_a=0.5$ sec.; Beam rate time constant $T_r=10$ sec.;

Noise filter time constant $T_n=0.73$ sec.; Aircraft blind landing system azimuth displacement demand = Y_i feet; Aircraft blind landing system azimuth displacement = Y_o feet; The resultant zero-velocity lag system is derived as in [18]. $G(s) =$

$$\frac{0.097+0.965s}{0.097+0.965s+5.143s^2+13.833s^3+13.851s^4+6.110s^5+s^6}$$

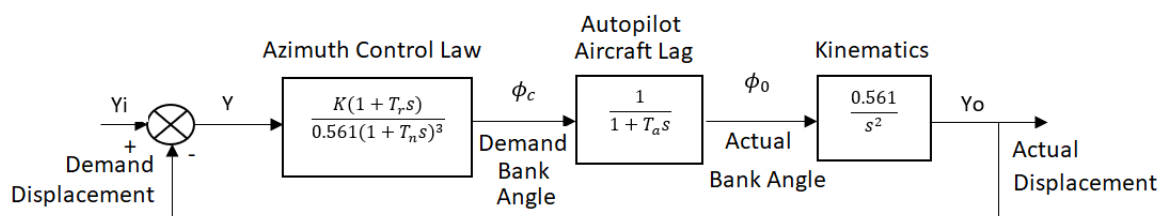


Fig. 11 Aircraft Azimuth Channel Blind Landing System

The given aircraft blind landing system shows lag in the step response. Hence the second order reduced model to be designed is accounted with a lag component and the reduced order model becomes $R(s) = e^{-\tau s} \frac{K_1 s + SS(L_0)}{s^2 + L_1 s + L_0}$. The lag component is substituted by its first order Pade

approximation $e^{-\tau s} = \frac{1-\frac{\tau}{2}s}{1+\frac{\tau}{2}s}$ [19]. The K_1 , L_0 , L_1 and τ values are obtained by WOA with CF for minimum ISE.

Figure 12 and Table IV shows the comparable results by the proposed method.

Table. 4 ISE Comparison of Reduced Order Models - Example 3

Method	Reduced Order Model	ISE
Marshall model with lag [18]	$R(s) = \frac{0.0126 + 0.1081s - 0.1789s^2}{0.0126 + 0.1076s + 0.5071s^2 + s^3}$	0.3095
Proposed Method	$R(s) = e^{-3.0018s} \frac{0.2592s + 0.0357}{s^2 + 0.1726s + 0.0357}$	0.4255

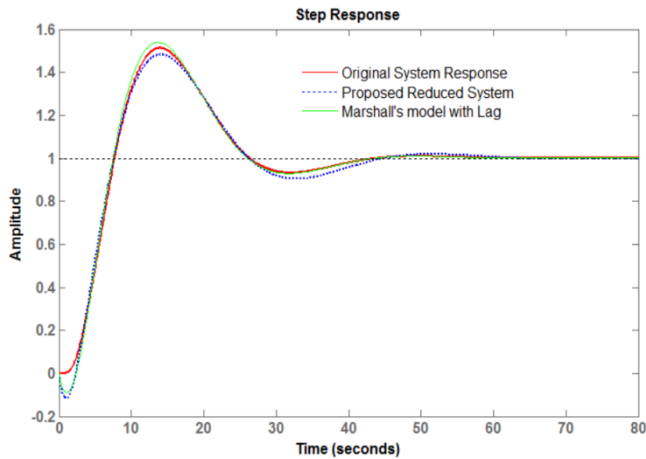


Fig. 12 Step response comparison of Aircraft Blind Landing System

D. Example 4

A simplified model of a single synchronous generator connected to an infinite bus through a large transmission line is considered from [20] as shown in Figure 13.

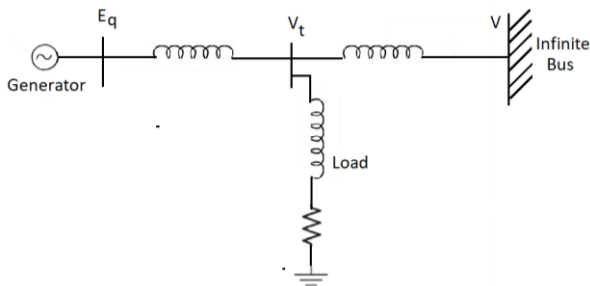


Fig. 13 Single Synchronous Generator Connected to an Infinite Bus.

The given single machinepower system'smodelling and design details are referred from [20]. The dynamic state equation and the numeric data of the given power system are:

$$\begin{bmatrix} \Delta \dot{E}_q \\ \Delta \dot{\delta} \\ \dot{\omega} \\ \dot{P} \\ \dot{P}_1 \end{bmatrix} = \begin{bmatrix} -\frac{1}{T_{do}b_2} & 0 & \frac{c_2}{b_2} & 0 & 0 \\ 0 & 0 & 1 & \frac{1}{M} & 0 \\ -\frac{b_1}{M} & -\frac{c_1}{M} & -\frac{D}{M} & \frac{1}{M} & 0 \\ 0 & 0 & 0 & 0 & 1 \\ 0 & 0 & -\frac{c}{a} & -\frac{1}{a} & -\frac{b}{a} \end{bmatrix} \begin{bmatrix} \Delta E_q \\ \Delta \delta \\ \omega \\ P \\ P_1 \end{bmatrix} + \begin{bmatrix} 1 \\ 0 \\ 0 \\ 0 \\ 0 \end{bmatrix} U$$

Where Moment of inertia $M=1.0$;

Excitation voltage of the machine $E_q=1.482$; Electrical output power of the machine $P=2.105$; Direct axis field time constant $T_{do} = 5\text{sec.}$; Self admittance of the network at the internal bus of the machine $y_{11}=0.266-j1.530$; Mutual admittance of the network between internal bus of the machine and infinite bus $y_{12}=0.180+j1.080$; Damping coefficient of the machine $D=0.5$; rotor angle in electrical radians $\delta^0 = 60^\circ$; $a=T_1T_2=0.05$; $b=T_1+T_2=0.6$; $c=0.05$; Direct axis synchronous reactance $x_d=0.32$; Direct axis transient reactance of the machine $x'_d = 0.084$; $T_1=0.1\text{sec.}$; $T_2=0.5\text{ sec.}$ T_1 and T_2 are time constants of prime-mover governor. For the change in voltage and rotor angle, the transfer function matrix is given as

$$[G(s)] = \begin{bmatrix} G_{11}(s) \\ G_{21}(s) \end{bmatrix} = \begin{bmatrix} \frac{s^4 + 12.5s^3 + 26.57s^2 + 17.84s + 11.4}{s^5 + 12.68s^4 + 29.27s^3 + 27.65s^2 + 22.9s + 2.086} \\ \frac{-1.815s^2 - 21.78s - 36.3}{s^5 + 12.68s^4 + 29.27s^3 + 27.65s^2 + 22.9s + 2.086} \end{bmatrix}$$

For the given higher order MIMO system, the second order reduced models attained by the proposed method are

$$R_{11}(s) = \frac{s + 0.8794}{s^2 + 1.7093s + 0.1609} \text{ and } R_{21}(s) = \frac{2.1429s - 4.7830}{s^2 + 2.7125s + 0.2749}$$

Table. 5 ISE Comparison of Reduced Order Models - Example 4

Method	Reduced Order Model	ISE
Nidhi model [20]	$\begin{bmatrix} R_{11}(s) \\ R_{21}(s) \end{bmatrix} = \begin{bmatrix} \frac{2.056s + 1.19}{s^2 + 2.755s + 0.2178} \\ \frac{5.914s - 4.338}{s^2 + 1.999s + 0.2493} \end{bmatrix}$	$\begin{bmatrix} 17.1724 \\ 205.2841 \end{bmatrix}$
Proposed Method	$\begin{bmatrix} R_{11}(s) \\ R_{21}(s) \end{bmatrix} = \begin{bmatrix} \frac{s + 0.8794}{s^2 + 1.7093s + 0.1609} \\ \frac{2.1429s - 4.7830}{s^2 + 2.7125s + 0.2749} \end{bmatrix}$	$\begin{bmatrix} \mathbf{0.8168} \\ \mathbf{11.3284} \end{bmatrix}$

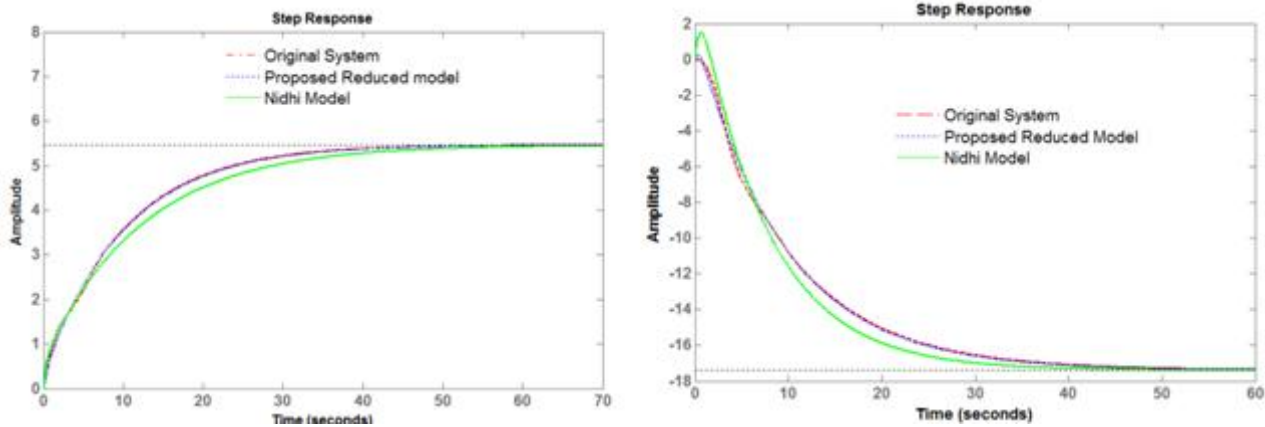


Fig. 14 Step response comparison of $R_{11}(s)$ and $R_{12}(s)$ – Example 4

Table V and Figure 14 justify the efficacy of the proposed method when compared to the existing model [20].

VI. CONCLUSION

The Constriction factor that was developed to prevent the explosion in swarm intelligence technology is adopted in this work to enhance the WOA which involves random search exploration as well. The better convergence demonstrated by WOA with CF influences the implementation of it in minimization of ISE in lower order modelling. The amplitude matching technology and WOA with CF are integrated to determine the unknown parameters of second order reduced models of LTICS and LTIDS. The proposed method is implemented to real time digital filter, Aircraft blind landing system and MIMO power system models with comparable results.

REFERENCES

1. Mirjalili, S & Lewis, A, 'The Whale Optimization Algorithm', Advances in Engineering Software, pp. 51-67, 2016.
2. Kennedy, J & Eberhart, R, 'Particle Swarm Optimization', Proceedings of the 1995 IEEE International Conference on Neural Networks, IEEE Press, pp. 1942-1948, 1995.
3. Hu, H & Xu, YB, 'A Whale Optimization Algorithm with Inertia Weight', WSEAS Transactions on Computers, pp. 319-326, 2016.
4. Jangir, P & Indrajit, NT, 'A Novel Adaptive Whale Optimization Algorithm for Global Optimization', Indian Journal of Science and Technology, 2016.
5. Sivalingam, R, Chinnamuthu, S and Das, SS, 'A Modified Whale Optimization Algorithm-Based Adaptive Fuzzy Logic PID Controller for Load Frequency Control of Autonomous Power Generation Systems', Automatika, pp. 410-421, 2018.
6. Clerc, M and Kennedy, J, 'The Particle Swarm—Explosion, Stability, and Convergence in a Multidimensional Complex Space', IEEE Transactions on Evolutionary Computation, vol. 6, pp. 58-73, 2002.
7. Lim, S, Montakhab, M & Nouri, H, 'A constriction factor based particle swarm optimization for economic dispatch', The 2009 European Simulation and Modelling Conference (ESM2009), Leicester, United Kingdom, 2009.
8. Biswas, S & Mandal, KK, 'Constriction Factor Based Particle Swarm Optimization for Analyzing Tuned Reactive Power Dispatch', Frontiers in Energy, Springer Link, vol. 7, no. 2, pp. 174-181, 2013.
9. Dieu, VN, Dung, LA & Khai, NP, 'Particle Swarm Optimization with Constriction Factor for Optimal Reactive Power Dispatch', GMSARN International Journal, no. 7, pp. 31-40, 2013.
10. Innocente, MS & Sienz, J, 'Particle Swarm Optimization with Inertia Weight and Constriction Factor', International Conference on Swarm Intelligence, Cergy, France, 2011.
11. N.Malathi, N.Devarajan, "A Simple Order Reduction Scheme for Multi Input Multi Output Linear Time Invariant Systems", International Journal of Pure and Applied Mathematics, Vol.118 No.10, pp.115-122, 2018.
12. N.Malathi, N.Devarajan, "A Simplified Approach to Reduced Order Modelling of Linear Time Invariant Systems using Amplified Matching with PSO", Journal of Advanced Research in Dynamical and Control Systems, Special Issue-13, pp.1714-1723, 2018.
13. Ramesh, K, Nirmalkumar, A & Gurusamy, G, 'Design of Digital IIR filters with the Advantages of Model Order Reduction Technique', World Academy of Science, Engineering and Technology International Journal of Electronics and Communication Engineering, pp. 1010-1015, 2009.
14. Gomathi, P, 'Certain Algebraic Schemes For Second Order Model Formulation And Applications In Linear Time Invariant Systems', 2014. http://shodhganga.inflibnet.ac.in/bitstream/10603/23887/1/11_chapter%206.pdf
15. Parmer, G, Muckerjee, S & Prasad, 'Reduced Order Modelling of Linear MIMO Systems using Genetic Algorithm', Int. J. Simul. Model, pp. 173-184, 2007.
16. Vishwakarma, C & Prasad, R, 'Order reduction using the advantages and differentiation method and factor division algorithm', Indian Journal of Engineering and Material Sciences, vol. 15, pp. 447-451, 2008.
17. Salma, U & Vaisakh, K, 'Reduced Order Modeling of Linear MIMO Systems Using Soft Computing Techniques', SEMCCO 2011, Part II, LNCS 7077, Verlag Berlin Heidelberg: Springer, pp. 278-286, 2011.
18. Manoj Kumar Jaiswal, "Application of Modelling and Order Reduction in Aircraft Instrumentation system", University of Roorkee, 1990. <http://shodhbhagirathi.iitr.ac.in:8081/jspui/image/pdf/web/viewer.htm?file=/jspui/bitstream/123456789/12599/1/EED245281.pdf>
19. Aidan O' Dwyer, "The Estimation and Compensation of Processes with Time Delays", Dublin City University, 1996. http://doras.dcu.ie/19217/1/Aidan_O'Dwyer_20130621142123.pdf
20. Nidhi Singh, "Reduced Order Modelling and Controller Design", Indian Institute of technology Roorkee, 2007 <http://shodhbhagirathi.iitr.ac.in:8081/jspui/image/pdf/web/viewer.htm?file=/jspui/bitstream/123456789/1841/1/REDUCED%20ORDER%20MODELLING%20AND%20CONTROLLER%20DESIGN.pdf>